Corrosion Inhibitory Evaluation of Indole-3-Carbaldehyde 4-Methyl-3-Thiosemicarbazone on Mild Steel: Weight Loss, Langmuir Isotherm, SEM-EDX and DFT Analysis

**Intan Syahirah Abdul Salam[2], Sheikh Ahmad Izaddin Sheikh Mohd Ghazali[1,2],
Siti Syaida Sirat[2,3] and Nur Nadia Dzulkifli[1,2]***

[1]Material, Inorganic, and Oleochemistry (MaterInOleo) Research Group, School of Chemistry and Environment,
Faculty of Applied Sciences, Universiti Teknologi MARA Cawangan Negeri Sembilan, Kampus Kuala Pilah,
Pekan Parit Tinggi, 72000 Kuala Pilah, Negeri Sembilan, Malaysia
[2]School of Chemistry and Environment, Faculty of Applied Sciences, Universiti Teknologi MARA Cawangan
Negeri Sembilan, Kampus Kuala Pilah, Pekan Parit Tinggi, 72000 Kuala Pilah, Negeri Sembilan, Malaysia
[3]Atta-ur-Rahman Institute for Natural Product Discovery (AuRIns), Universiti Teknologi MARA,
Kampus Puncak Alam, 42300 Bandar Puncak Alam, Selangor, Malaysia
*Corresponding author (e-mail: nurnadia@uitm.edu.my)

Corrosion has been discovered to degrade metal surfaces in acidic media. In-situ synthesis of indole-3-carbaldehyde 4-methyl-3-thiosemicarbazone [ICar4MTSC] as a corrosion inhibitor was carried out. The predicted structure of ICar4MTSC was supported by elemental analysis, melting point, FT-IR, UV-Vis, and NMR analysis. To assess the efficacy of ICar4MTSC, weight loss was conducted in an acidic environment (1M HCl). The results revealed that as its concentration increases, so does the corrosion inhibition's performance. The $R^2 = 1$ value of the Langmuir adsorption isotherm pointed out that the ICar4MTSC designed a monolayer on the mild steel surface and interacted with the adsorbed inhibitors. The Gibbs free energy value: ΔG_{ads} = -21.9873 kJ mol^{-1} implies that the ICar4MTSC displayed both forms of adsorption types (chemisorption and physisorption). The surface morphology of mild steel at its highest concentration (0.5 μM) that had been soaked in 1M HCl for 24 hours was imaged using SEM-EDX and mapping. The results deduced that a protective layer of ICar4MTSC (0.5 μM) was created, resulting in a smoother surface. Whereas the rough and pitting surface on the mild steel denotes the absence of ICar4MTSC (blank). The DFT (intrinsic molecular characteristics and MEP) analysis showed that the ICar4MTSC contains promising adsorption sites (C=S, N atoms of the thiosemicarbazide moiety, and the benzene of the indole ring) which could potentially adsorb the mild steel surface by chemisorption and physisorption.

Keywords: Thiosemicarbazone; HCl; weight loss; DFT; Langmuir isotherm

Corrosion is a frequently used term referring to a natural phenomenon throughout industries that causes environmental pollution and property loss. The depreciation of a metal arises through its chemical reaction with environmental factors such as oxygen, hydrogen, or bacteria [1]. Unending corrosion processes generate a stressful environment on the metal surfaces of bridges, buildings, and pipelines that leads to fracture [2, 3]. The destruction created by corrosion activity can be fended off with simple initiatives and methods [4]. A corrosion inhibitor aids in intensifying the metal's resistance to corrosion processes at low concentrations. In corrosive media, a simple strategy for generating a protective layer by applying inhibitors to minimise the rate of corrosion can be used [5, 6]. The azomethine (C=N) and thione (C=S) moieties in thiosemicarbazone are responsible for generating an adsorption layer on metal surface [7].

The effectiveness of thiosemicarbazone as a corrosion inhibitor can be correlated to its intrinsic molecular characteristics using density functional theory (DFT) calculations [9]. This might clarify the mechanisms underpinning ligand adsorption and corrosion inhibition and provide a design guide for new ligands with corrosion-prevention properties. Furthermore, the polar region of organic inhibitor compounds featuring heteroatoms has the potential to form an adsorption film [8]. Although the compound has been synthesised and characterised with X-ray crystallography [10], there are yet no studies on its corrosion inhibition activity. Besides that, many compounds have been studied for their potential as corrosion inhibitors, but fundamental research to find an excellent inhibitor still needs to be done. Therefore, the goal of this study is to synthesise, characterise, and assess the potential of ICar4MTSC as a corrosion inhibitor. The corrosion inhibition performances in

11 Intan Syahirah Abdul Salam, Sheikh Ahmad
    Izaddin Sheikh Mohd Ghazali, Siti Syaida
    Sirat and Nur Nadia Dzulkifli

Corrosion Inhibitory Evaluation of Indole-3-Carbaldehyde
4-Methyl-3-Thiosemicarbazone on Mild Steel: Weight,
Loss, Langmuir Isotherm, SEM-EDX and DFT Analysis

HCl were reviewed using the weight loss technique and surface analysis by SEM-EDX with mapping. The Langmuir isotherm and Gibbs energy were computed, and a DFT analysis was carried out to theoretically look at the structure-reactivity relationship of the corrosion inhibitor. The chosen study technique can yield enlightening results concerning the efficacy of the studied compound as an acid corrosion inhibitor.

EXPERIMENTAL

Materials and Characterisation

The chemicals namely 4-methyl-3-thiosemicarbazide (97%) and indole-3-carbaldehyde (97%) were purchased from Sigma-Aldrich. The elemental data (CHNS) of ICar4MTSC was derived using the Elemental Analyser Model Vario EL Cube. The melting point of ICar4MTSC was measured using the melting point apparatus model SMP10 Stuart. Next, the fingerprints of ICar4MTSC were determined using FTIR with the Perkin Elmer Model GX (650 cm^{-1} to 4000 cm^{-1}). The structure of ICar4MTSC was ascertained using a Lambda JEOL 400 MHz NMR with deuterated dimethyl sulfoxide (DMSO-d_6) as the solvent. A UV-Vis spectrometer was used to detect the electronic transitions (200 to 400 nm) in DMSO (1×10^{-4} M) using the PG instrument T80/T80+ spectrophotometer. Morphological study was utilised on mild steel (bare, blank, and 0.5 µM) using the SEM Zeiss Merlin model at 500x magnification.

The Synthesis of ICar4MTSC

ICar4MTSC was synthesised using the reflux method of condensation. ICar4MTSC was prepared by dropping the methanolic of 4MTSC (0.5258 g, 5 mmol) into the methanolic of ICar (0.7258 g, 5 mmol) [1:1]. The mixture was continuously stirred for 4 hours at close to 70 °C. The solution was cooled to room temperature after 4 hours, and the white precipitate was filtered before being washed with cold methanol. Lastly, it was desiccated on anhydrous silica gel, and the purity of the ICar4MTSC was verified by Thin Layer Chromatography.

Corrosion Inhibitory Studies

Preparation of Solution and Specimen

1 M of 37% HCl was prepared by dilution with distilled water. The concentrations of ICar4MTSC [0.1, 0.2, 0.3, 0.4, and 0.5 µM] were also prepared with distilled water. All the mild steel specimens (2 cm^2) were polished with a series of silica carbide papers from 320 to 1,200 grades. They were washed with distilled water and acetone [11].

Weight Loss Method

The polished specimen's initial weight was measured. It was then soaked in 1 M HCl with the presence and absence of ICar4MTSC at concentrations of (1, 2, 3, 4, and 5) x 10^{-1} M for 24 hours at 25 °C. After 24 hours, the specimen was cleaned with distilled water and acetone before drying. The specimen was re-weighed after drying to measure the final weight. The weight loss was calculated by subtracting the weight of the specimen before and after soaking. The weight loss in g/cm^2 was applied in the calculation of the percentage inhibitory efficacy (%IE) and surface coverage (θ) of the ICar4MTSC [12]. The corrosion rate (CR in g/cm^{2}h) was also computed using the following equation:

$$Corrosion\ rate\ (CR) = \frac{\Delta W}{st}$$

Where ΔW is the average weight loss, *s* is the total area of the specimen, and *t* is the soaking time in hours. The weight loss technique was repeated in triplicates.

Langmuir Isotherm and Gibbs Energy

The Langmuir adsorption isotherm approximated the maximum surface coverage adsorption of ICar4MSTC as concentrations rose. The degree of surface coverage (θ) was utilised to identify the most effective type of adsorption isotherm that matched the predicted corrosion rate values from the weight loss technique data [13]. Using the weight loss data, a linear graph was constructed to plot C/θ versus C. Based on the plotted graph, the following equations were used:

$$\frac{Cinh}{\theta} = \left(\frac{1}{Kads}\right) x\ Cinh$$

$$\theta = \frac{C°RW - CRW}{C°RW}$$

$$\%IE = \frac{C°RW - CRW}{C°RW} X\ 100$$

Where:

θ = the fractional surface coverage

C$_{inh}$ = the ICar4MTSC concentration

K$_{ads}$ = the equilibrium constant of the adsorption process

C°$_{RW}$ = the corrosion rate in the absence of ICar4MTSC

C$_{RW}$ = the corrosion rate in the presence of ICar4MTSC

%IE = corrosion inhibition efficiency

The Gibbs Energy was computed using the following equation:

$$\Delta G = -RTln(55.5\ x\ K_{ads})$$

Where;

G = Gibbs Free Energy

12 Intan Syahirah Abdul Salam, Sheikh Ahmad
Izaddin Sheikh Mohd Ghazali, Siti Syaida
Sirat and Nur Nadia Dzulkifli

Corrosion Inhibitory Evaluation of Indole-3-Carbaldehyde
4-Methyl-3-Thiosemicarbazone on Mild Steel: Weight,
Loss, Langmuir Isotherm, SEM-EDX and DFT Analysis

T = Temperature in Kelvin (K)

R = Gas constant, 8.314 JK^{-1} mol^{-1}

K_{ads} = Adsorption rate (data obtained from Langmuir Isotherm)

Scanning Electron Microscopy (SEM) – Energy Dispersive X-ray (EDX) with Mapping

The SEM-EDX with mapping was utilised to generate surface morphological images of the bare polished specimen and the specimen in the highest concentration of ICar4MTSC after 24 hours of immersion in 1 M HCl [14]. The equipment provides topographical and elemental information shown on the specimen surfaces.

Density Functional Theory (DFT)

The DFT investigation was carried out using Gaussian09 utilising the hybrid functional RB3LYP method 6-31G(d,p) basis set to optimise the Icar4MTSC structure without symmetry constraints [15, 16]. The RB3LYP method consists of Becke's three parameter (B3) hybrid exchange functional in conjunction with the correlation functional of Lee Yang and Parr (LYP) [17]. GaussView 5.0 was applied to visualise the results of the DFT.

RESULTS AND DISCUSSION

Physiochemical Analysis

Table 1 shows the physiochemical characteristics of the ICar4MTSC, including elemental content (%), colour, and melting point. The melting point of ICar4MTSC is between 215-217°C [18], indicating that as the number of bonds increases, more energy is required to transition between phases. The elemental percentages of C, H, N, and S for the obtained white precipitate were in good alignment with the computed values. Figure 1 depicts the proposed structure of the ICar4MTSC.

Table 1. The physicochemical characteristic and elemental analysis of ICar4MTSC.

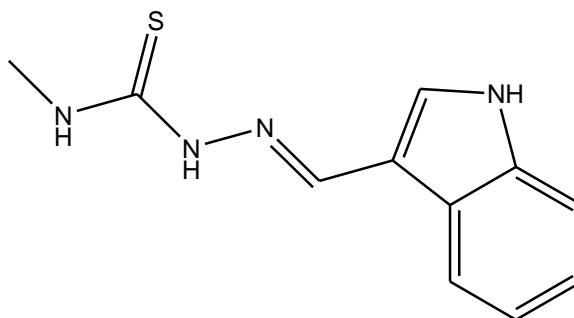| Color	Melting point (°C)	Elemental analysis (Experimental) (%)			
		C	H	N	S
White precipitate	215-217	58.17 (56.87)	5.14 (5.21)	23.07 (24.12)	12.70 (13.80)

*( ) Calculated values

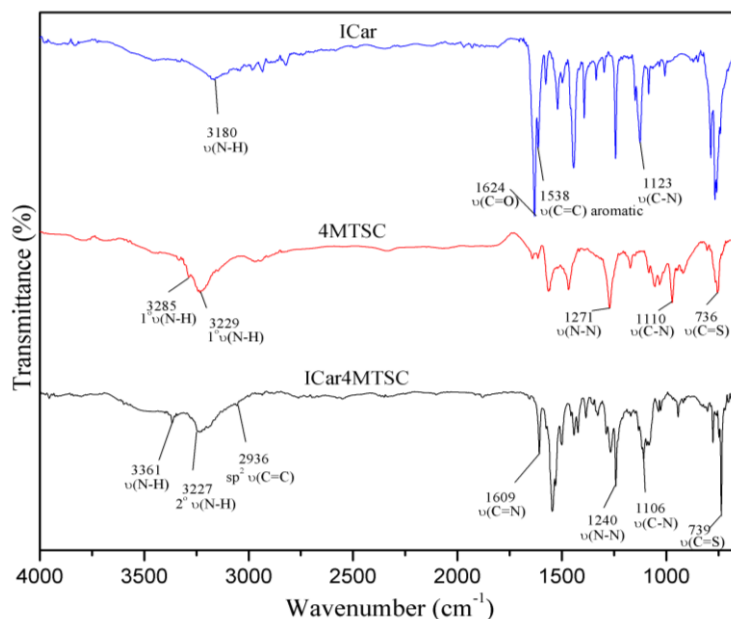**Figure 1.** The suggested structure of ICar4MTSC.

Figure 2. ATR-FTIR spectra of ICar, 4MTSC and ICar4MTSC.

FTIR Analysis

The raw materials [ICar, 4MTSC] and ICar4MTSC were portrayed by ATR-FTIR spectroscopy which displayed several notable stretching bands as fingerprints as shown in Figure 2. No stretching band was presented for the thiol group ν(S-H) within 2500-2600 cm^{-1}, highlighting that the ICar4MTSC is in thione form when in solid state [19, 20]. The aldehyde, ν(C=O) [ICar] and primary amine, ν(1 NH_2) [4MTSC] stretching bands are noticeable at 1624 cm^{-1} and 3229, 3285 cm^{-1}, respectively. The functional groups were removed completely in the ICar4MTSC and replaced by intense azomethine nitrogen, ν(C=N) (1609 cm^{-1}) [21, 22]. The thiocarbonyl stretching band ν(C=S) emerged at 739 cm^{-1} [ICar4MTSC]. These transformations verified the formation of ICar4MTSC. Lastly, stretching bands of ν(N-N) appeared at 1271 cm^{-1} [4MTSC] and 1242 cm^{-1} [ICar4MTSC] [23].

1H and 13C NMR

The NMR values are tabulated in Table 2. The 1H-NMR spectrum gives information on the protons contained within ICar4MTSC as well as the environmental features of the hydrogen protons [24]. At $\delta = 11.14$ ppm, a singlet of N-H proton emerges at a greater chemical shift (downfield) generated by the de-shielding of the heteroatoms S and N. At $\delta = 8.31$ ppm, a singlet peak representing the HC=N proton signal was spotted and de-shielded by the N atom [25, 26]. The presence of electronegative atoms connected to the N-H and HC=N systems
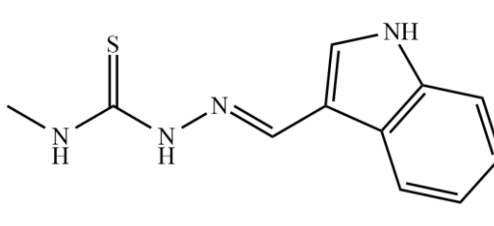
reduce the electron densities surrounding the protons, resulting in reduced shielding. The peaks at $\delta = 7.79$ and $\delta = 7.13$-7.44 ppm were spotted and correlated to the C-H of the indole and benzene rings, respectively. The N-H proton of the indole ring was visible at 11.57 ppm. The methyl group, (-CH_3) and NH-C(S), which appeared as doublet and singlet small peaks, were ascribed to the upfield regions in the spectrum at 3.09, 3.08 ppm and 2.50 ppm, respectively.

The 13C NMR signals of ICar4MTSC, which were detected downfield at $\delta = 177.26$ and 140.94 ppm, signify the presence of C=S and C=N, respectively. The C=S and C=N were the most de-shielded, owing to considerable electron delocalisation and the conjugated structure of the rings, thereby lowering the electron density surrounding the carbon atom [27]. The terminal methyl CH_3 emerged at 31.48 ppm, as it was directly bonded to the electronegative atom, N-H. The aromatic ring, however, revealed six distinct peaks at chemical shifts of 112.19, 121.00, 122.66, 123.09, 124.42, and 137.50 ppm. Meanwhile, the indole ring revealed 2 distinct peaks at 131.22 and 137.50 ppm.

UV-Visible

The absorption peaks for ICar4MTSC in DMSO (1x10^{-4} M) emerged between 200 and 400 nm, as illustrated in Figure 3. The azomethine, C=N, and rings (indole and aromatic) were assigned to the ICar4MTSC's two primary absorption peaks, which were observed at 267 ($\pi \rightarrow \pi^*$) and 361 ($n \rightarrow \pi^*$) nm, respectively [28, 29].

14 Intan Syahirah Abdul Salam, Sheikh Ahmad Izaddin Sheikh Mohd Ghazali, Siti Syaida Sirat and Nur Nadia Dzulkifli

Corrosion Inhibitory Evaluation of Indole-3-Carbaldehyde 4-Methyl-3-Thiosemicarbazone on Mild Steel: Weight, Loss, Langmuir Isotherm, SEM-EDX and DFT Analysis

Table 2. ^{1}H and ^{13}C NMR data of ICar4MTSC.

Spectra	Chemical shift (ppm)	Type of proton or carbon	Structure of ICar4MTSC
^{1}H NMR	2.50 (s)	CH$_3$-<u>NH</u>-C(S)	
	7.13 - 7.23 (m)	C-H aromatic	
	7.42 -7.44 (m)	C-H aromatic	
	7.79 (d)	C=<u>CH</u>-NH ring	
	3.08, 3.09 (d)	<u>CH$_3$</u>-NH-C(S)	
	8.26 – 8.28 (m)	C-H aromatic	
	8.31 (s)	<u>CH</u>=N	
	11.14 (s)	N-H aliphatic	
	11.57 (s)	N-H ring	
^{13}C NMR	31.48	-<u>CH$_3$</u>	
	111.65	N=C-<u>C</u>=C	
	112.19, 121.00, 122.66, 123.09, 124.42	Aromatic	
	131.22	C=<u>C</u>-NH (ring)	
	137.50	NH-<u>C</u>-C=C ring	
	140.94	C=N	
	177.26	C=S	
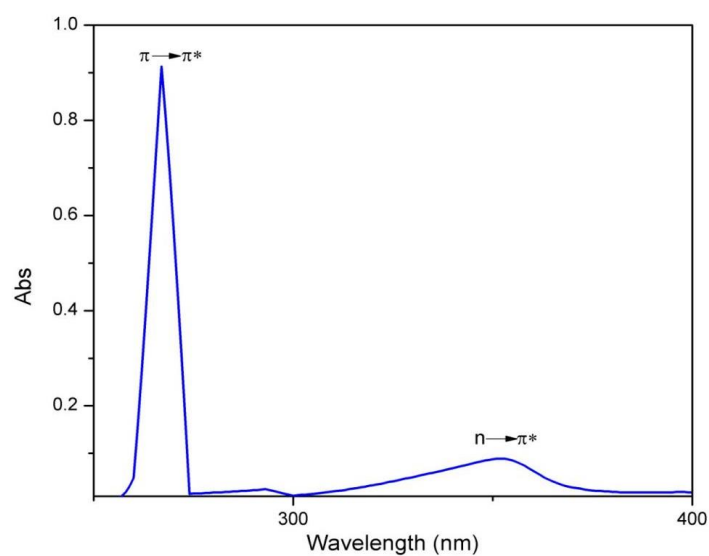
Figure 3. UV-Vis absorption spectrum of ICar4MTSC.

15   Intan Syahirah Abdul Salam, Sheikh Ahmad Izaddin Sheikh Mohd Ghazali, Siti Syaida Sirat and Nur Nadia Dzulkifli

Corrosion Inhibitory Evaluation of Indole-3-Carbaldehyde 4-Methyl-3-Thiosemicarbazone on Mild Steel: Weight, Loss, Langmuir Isotherm, SEM-EDX and DFT Analysis

Table 3. Weight loss data measurement.

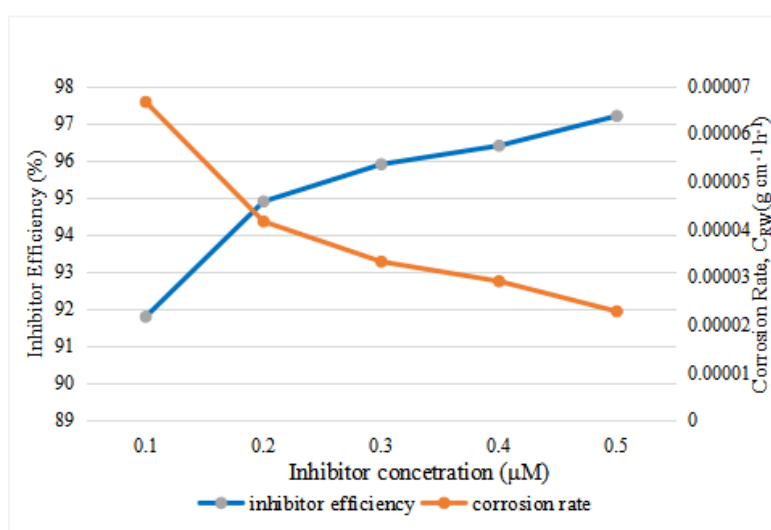| Acid	Concentration (ppm)	Weight loss, ΔW (g)	Corrosion rate, C_{RW} (g cm^{-2} h^{-1})	Surface coverage, θ	Inhibition efficiency, $\eta\%$
1 M HCl	blank	0.0393	8.1800 x 10^{-4}	-	-
	0.10 μM	0.0032	6.6700 x 10^{-5}	0.9186	91.8
	0.20 μM	0.0020	4.1700 x 10^{-5}	0.9491	94.9
	0.30 μM	0.0016	3.3300 x 10^{-5}	0.9593	95.9
	0.40 μM	0.0014	2.9200 x 10^{-5}	0.9644	96.4
	0.50 μM	0.0011	2.2900 x 10^{-5}	0.9720	97.2

Figure 4. Inhibition efficiency and corrosion rate of ICar4MTSC at different concentrations immersed in 1 M HCl solution.

Corrosion Inhibitory Study

Weight Loss Technique

The capability of the ICar4MTSC as an inhibitor that retards the corrosion rate on mild steel exposed to corrosive HCl solution was assessed by employing the weight loss method [30]. Weight loss, commonly known as the coupon method, is the most straightforward and long-established way of assessing corrosion. The weight loss measurements collected after a 24-hour soak in HCl at 25°C (room temperature) were used to scrutinise the influence of ICar4MTSC concentration on corrosion inhibition effectiveness. Based on the data collected in Table 3 and Figure 4, the result depicts that the corrosion protection effectiveness of the inhibitor increased proportionally with the increase in ICar4MTSC concentrations [31, 32], and that the highest efficiency was obtained at 0.50 μM (97.2 %). The data imply that as concentration increases, more ICar4MTSC is adsorbed on the mild steel surface, assisting in the protection of a larger surface area and the creation of a barrier film between two phases (corrosive agent and mild steel surface).

Langmuir Adsorption Isotherm Study

An overview of the adsorption mechanism could be provided by studies of the adsorption of ICar4MTSC to mild steel surfaces employing adsorption isotherms [33]. The most efficient way to describe the adsorption behaviour of ICar4MTSC was found to be the Langmuir adsorption isotherm, as shown in Figure 5, namely by substituting the weight loss values for the Langmuir isotherm calculation. The slope and the corrosion rate inhibitors had the best correlation, and the ICar4MTSC created a monolayer adsorbed on the mild steel surface. According to the Langmuir isotherm, a hard surface of mild steel contains a fixed number of adsorption sites, each with a specific adsorption species [34].
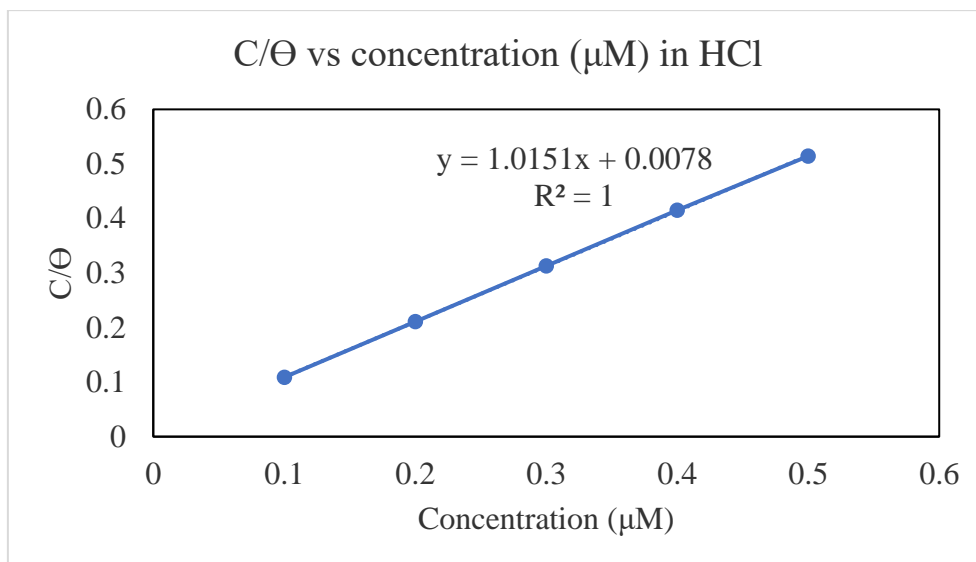
16   Intan Syahirah Abdul Salam, Sheikh Ahmad
     Izaddin Sheikh Mohd Ghazali, Siti Syaida
     Sirat and Nur Nadia Dzulkifli

Corrosion Inhibitory Evaluation of Indole-3-Carbaldehyde
4-Methyl-3-Thiosemicarbazone on Mild Steel: Weight,
Loss, Langmuir Isotherm, SEM-EDX and DFT Analysis

C/Ө vs concentration (µM) in HCl

$$y = 1.0151x + 0.0078$$
$$R^2 = 1$$

C/Ө (y-axis) vs Concentration (µM) (x-axis)

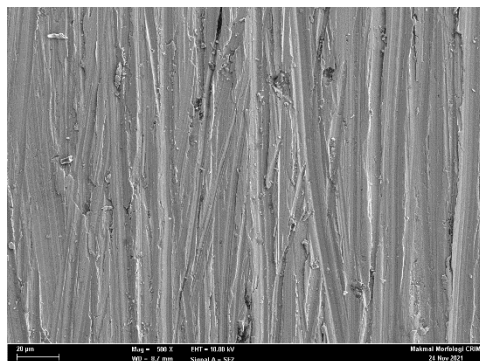**Figure 5.** Langmuir isotherm of ICar4MTSC in HCl.

Thermodynamic Calculation

A thermodynamic model was utilised to figure out the kind of adsorption of ICar4MTSC on the surface of the mild steel. The crucial value for computing the Gibbs free energy is the adsorption energy, K_{ads} = 128.21. The computed value of Gibbs free energy, G_{ads} = -21.987 kJ mol^{-1}, falls between -20 and -40 kJmol^{-1}. It was deduced that ICar4MTSC interacts with Cl$^-$ and Fe(II) ions on the mild surface via physisorption and chemisorption. However, the predicted value is close to -20 kJmol^{-1}, indicating that the process is primarily physisorption. Physisorption, often known as physical adsorption, is an exothermic process. According to the negative value of ΔG_{ads}, the process appears to be spontaneous, signifying that the inhibitors are successfully adsorbed on the mild steel surface. Water molecules and metal surfaces engage electrostatically during adsorption, which is followed by chemical interactions between the metal surface and the ICar4MTSC (inhibitor) [35]. All weak electrostatic interactions, including the Van Der Waals interactions, dipole-dipole forces, and London forces, are together referred to as "physisorption". The physisorption occurred between the protonated N$^+$ of ICar4MTSC and the chloride ion, Cl$^-$, through electrostatic interaction with the mild steel surface. HCl is referred to as a hydrogen ion (proton) donor in the Bronsted-Lowry theory that is able to interact with amine [34]. This interaction occurs when the amine is converted to a positively charged state. The physisorption shows the weakest interaction and is easily de-adsorbed. Meanwhile, through the sharing or transfer of electrons, chemisorption develops when the ICar4MTSC is covalently attached to the mild steel surface. A coordinative bond is created as a result of the transfer of lone pair electrons from S to the empty *d*-orbital of
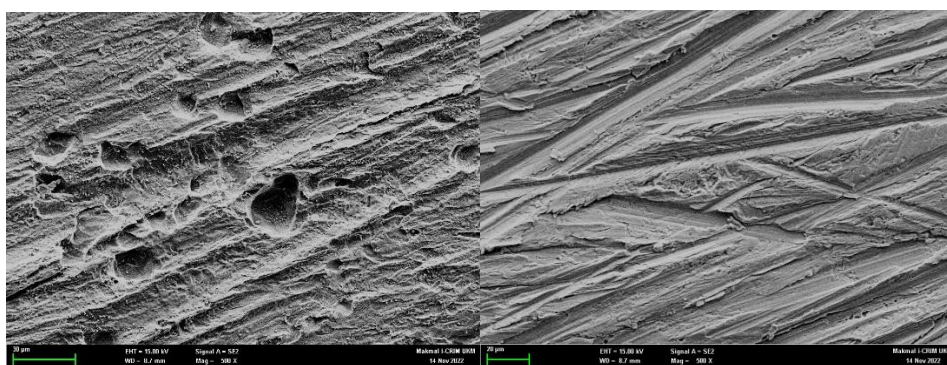
a mild steel surface. This interaction is aligned with the MEP.

Scanning Electron Microscopy with Energy Dispersive X-Ray (SEM-EDX)

SEM-EDX was utilised to explore the surface morphology of mild steel immersed in 1M HCl for 24 hours in the presence and absence of the inhibitor (ICar4MTSC). Figure 6 depicts the mild steel surface that was inspected at 500x magnification in the presence and absence of an inhibitor, respectively. Figure 6(a) displays the morphological image of a polished mild steel surface. Due to the unavoidable process of corrosion removal, silica carbide sheets formed apparent scratches on the mild steel surface. Meanwhile, Figure 6(b) depicts the mild steel exhibiting the corrosion situation that formed due to the rough surface and pitting on the surface of the mild steel immersed in 1 M HCl. Figure 6(c) shows the morphological image of mild steel in the presence of an inhibitor. As shown in Figure 6(c), adding 0.5 M ICar4MTSC to the corrosive solution alters the morphology of the mild steel, smoothing the surface and resulting in fewer cracks, proving the presence of a protective layer. The fact that the pits and cracks were not as obvious as they were on the blank implies that the mild steel was subjected to significantly less damage. The SEM analysis surmises that ICar4MTSC showed high inhibitory performance because it can create a protective layer by a mixed-adsorption mechanism that aligns with the Gibbs energy data [36-38]. Furthermore, the EDX analysis identified content on the mild steel surface to facilitate the creation of an adsorption layer by ICar4MTSC, as previously mentioned.

17   Intan Syahirah Abdul Salam, Sheikh Ahmad
Izaddin Sheikh Mohd Ghazali, Siti Syaida
Sirat and Nur Nadia Dzulkifli

Corrosion Inhibitory Evaluation of Indole-3-Carbaldehyde
4-Methyl-3-Thiosemicarbazone on Mild Steel: Weight,
Loss, Langmuir Isotherm, SEM-EDX and DFT Analysis

(a)

(b)   (c)

Figure 6. SEM images of mild steel surface: (a) of a polished mild steel, (b) immersed in 1 M HCl for 24 h, and (c) immersed in 1 M HCl with ICar4MTSC for 24 h.

Figure 7 depicts the elemental composition on the mild steel surface after 24 hours of immersion in 1 M HCl, proving the addition of two relatively small extra peaks indicating the presence of nitrogen (N) and sulphur (S) elements of ICar4MTSC. A low percentage weight of N and S was noticed in the mapping images [39]. The observation emphasised that the ICar4MTSC was unsymmetrical adsorbed on the mild steel surface. As noted in the Gibbs Energy section, the EDX images revealed that the ICar4MTSC had favourably adsorbed on the mild steel surface to minimise the corrosion rate by possibility chemisorption and physisorption.

Density Functional Theory

Intrinsic Molecular Characteristics

The computation based on the Density Functional Theory (DFT) was used to connect inhibitor efficiency in solid form with intrinsic molecular characteristics. The chemical stability and reactivity of the inhibitor structure were determined by key factors such as its highest occupied molecular orbital (HOMO), lowest unoccupied molecular orbital (LUMO), and energy band gap, as shown in Table 4. The thione component, C=S, had the most significant HOMO electron density distribution and the LUMO was distributed fairly equally along the thiourea moiety [40]. The HOMO

and LUMO of ICar4MTSC values were -5.2395 and -1.1652 eV, respectively. The high E_{HOMO} value highlighted the inhibitor's electron-donating capacity, which facilitates chemisorption on the metal surface [41]. In the meantime, it shows their larger propensity to receive electrons with low E_{LUMO} values from the metal surface. As a result, the energy gap ΔE between the HOMO and LUMO was calculated as 4.0743 eV.

The ICar4MTSC's DFT values were compared to those of a nearly comparable structure as studied by Ranwa et al. (2017) [42]. The low ΔE of ICar4MTSC signifies that the electron density transition from the HOMO→LUMO orbital is more reactive, implying that mild steel is better protected and favours high corrosion inhibition efficiency. A low E_{LUMO} value suggests that ICar4MTSC is more susceptible to accepting electrons from the metal surface via its thiourea moiety. Meanwhile, the high E_{HOMO} value denotes the electron-donating ability of C=S molecular orbitals, which aids in the adsorption process on the metal surface. The ionisation potential (I) of 5.2395 eV is higher than the electron affinity (A) of 1.1652 eV, displaying that ICar4MTSC prefers to release electrons rather than accept them. The global electrophilicity value is greater than 1.5 eV; hence, the ICar4MTSC could be suggested to possess strong electrophile properties [43].

18   Intan Syahirah Abdul Salam, Sheikh Ahmad
     Izaddin Sheikh Mohd Ghazali, Siti Syaida
     Sirat and Nur Nadia Dzulkifli

Corrosion Inhibitory Evaluation of Indole-3-Carbaldehyde
4-Methyl-3-Thiosemicarbazone on Mild Steel: Weight,
Loss, Langmuir Isotherm, SEM-EDX and DFT Analysis

Mapping Molecular Electrostatic Potential (MEP)

MEP is a reliable predictor of nucleophilic and electrophilic attack sites on the mild steel surface-based electron density distribution [44]. The thione group, C=S, is distinguished as a negative potential region (high electron density) and is responsible for the adsorption site on the mild steel surface. It often denotes the most favourable reactivity site for the electrophilic attack [45]. The N atoms of the thiosemicarbazide moiety and the benzene of the indole ring have a somewhat higher electron density surrounding them, which contributes to their capability of serving as adsorption sites. The pattern of MEP as shown in Figure 8 shows that the ICar4MTSC has the probability of adsorption on the mild steel surface through chemisorption-physisorption caused by the presence of many possible adsorption sites. On top of that, the hydrogen atoms have a very noticeable blue region (low electron density), which indicates a positive charge and the most desirable reactivity site for nucleophilic attack.
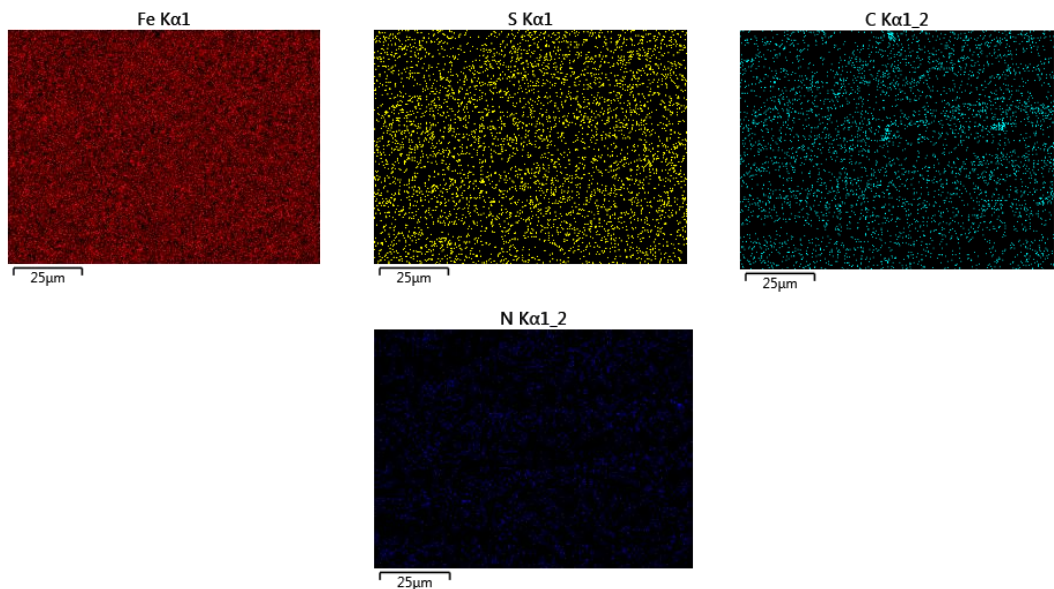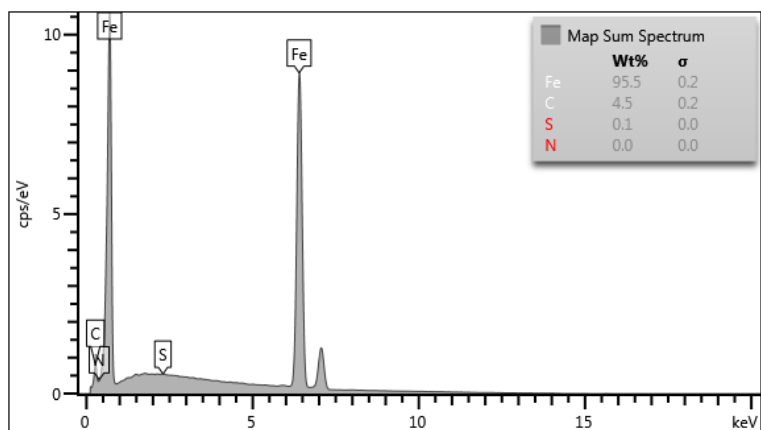

Figure 7. EDX mapping of element distribution on a mild steel surface after 24 hours immersion in 1 M HCl with a 5 M inhibitor.

19   Intan Syahirah Abdul Salam, Sheikh Ahmad
Izaddin Sheikh Mohd Ghazali, Siti Syaida
Sirat and Nur Nadia Dzulkifli

Corrosion Inhibitory Evaluation of Indole-3-Carbaldehyde
4-Methyl-3-Thiosemicarbazone on Mild Steel: Weight,
Loss, Langmuir Isotherm, SEM-EDX and DFT Analysis

Table 4. Comparison between HOMO, LUMO, energy gap (HOMO-LUMO), and related molecular properties of ICar4MTSC.

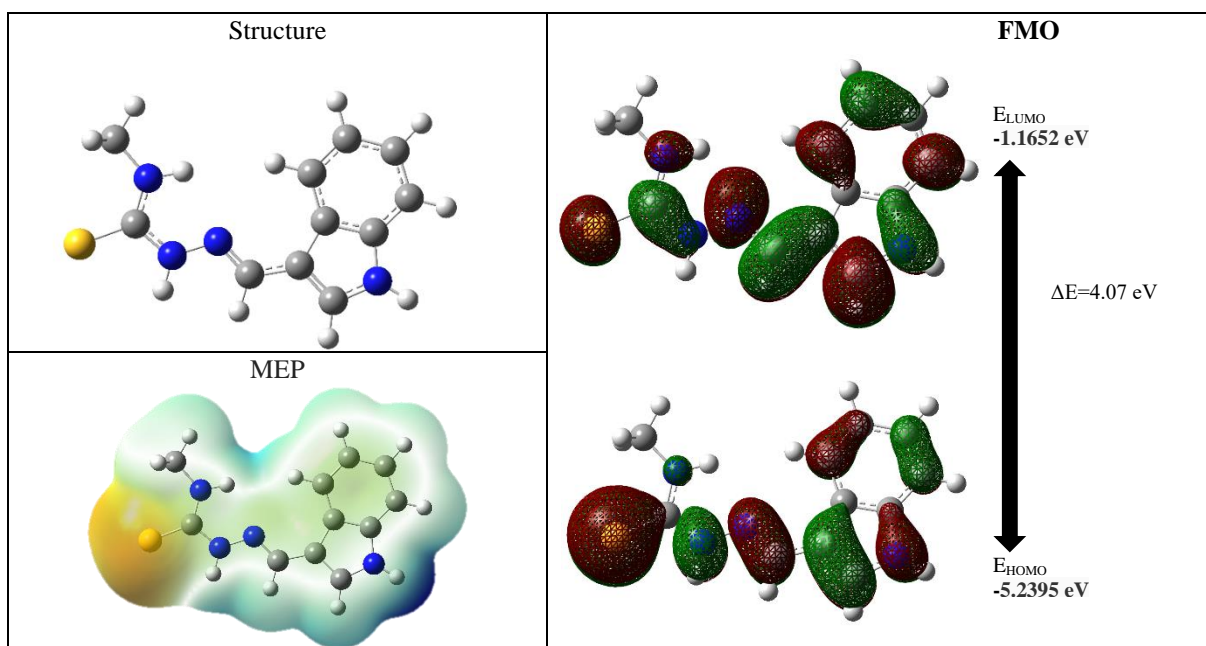| Molecular energy	ICar4MTSC
E_{HOMO}	-5.2395
E_{LUMO}	-1.1652
Energy gap (ΔE)	4.0743
Ionisation potential (I)	5.2395
Electron affinity (A)	1.1652
Global hardness (η)	2.0372
Softness (S)	0.4909
Chemical potential (μ)	-3.2024
Electronegativity (χ)	3.2024
Global electrophilicity (ω)	2.5170
Electron donating ability, (ω^-)	4.3728
Electron accepting ability, (ω^+)	1.1705

Figure 8. Optimised molecular structure, HOMO, LUMO, and MEP of 2ClAcTSC using DFT/B3LYP/6-31G (d,p).

CONCLUSION

The ligand, indole-3-carbaldehyde 4-methyl-3-thiosemicarbazone (ICar4MTSC), was successfully synthesised, and the proposed structure was verified using elemental analysis, FTIR, UV-Vis, and NMR spectroscopies. For the corrosion inhibition trial, the weight loss or coupon analysis demonstrated that as the ICar4MTSC concentrations [0.1, 0.2, 0.3, 0.4, and 0.5 µM] increased, so did its corrosion inhibition efficiency. The SEM-EDX with mapping morphology images of the mild steel surface confirmed that the ICar4MTSC had created an adsorption layer on the mild steel surface by a monolayer that deduced by Langmuir isotherm, resulting in a smoother surface. Overall, the ICar4MTSC exhibited anti-corrosion activity on the mild steel, providing good corrosion inhibition performance in 1 M HCl. Lastly, the DFT (Intrinsic molecular characteristics and MEP) deduced that the ICar4MTSC has the probability of adsorption

20   Intan Syahirah Abdul Salam, Sheikh Ahmad
Izaddin Sheikh Mohd Ghazali, Siti Syaida
Sirat and Nur Nadia Dzulkifli

Corrosion Inhibitory Evaluation of Indole-3-Carbaldehyde
4-Methyl-3-Thiosemicarbazone on Mild Steel: Weight,
Loss, Langmuir Isotherm, SEM-EDX and DFT Analysis

on the mild steel surface through chemisorption-physisorption caused by the presence of many possible adsorption sites.

ACKNOWLEDGEMENTS

REFERENCES

1. Al-Amiery, A. A., Al-Azzawi, W. K. and Wan Isahak, W. N. R. (2022) Isatin Schif base is an efective corrosion inhibitor for mild steel in hydrochloric acid solution: gravimetrical, electrochemical, and computational investigation. *Scientific Reports*, **12**, 17773–17790.

2. Valdez, B., Ramirez, J., Eliezer, A., Schorr, M., Ramos, R. and Salinas, R. (2016) Corrosion assessment of infrastructure assets in coastal seas. *Journal of Marine Engineering & Technology*, **15(3)**, 124–134.

3. Solmaz, R. (2014) Investigation of corrosion inhibition mechanism and stability of Vitamin B1 on mild steel in 0.5 M HCl solution. *Corrosion Science*, **81**, 75–84.

4. Hazani, N. N., Dzulkifli, N. N., Sheikh Mohd Ghazali, S. A. I. and Mohd, Y (2022) Synthesis, characterisation and corrosion inhibition of mild steel by butyltin(IV) 2-acetylpyridine 4-methyl-3-thiosemicarbazone in HCl. *Trends in Sciences*, **19(12)**, 1–18.

5. Patel, A. S., Panchal, V. A., Mudaliar, G. V. and Shah, N. K. (2013) Impedance spectroscopic study of corrosion inhibition of Al-Pure by organic schiff base in hydrochloric acid. *Journal of Saudi Chemical Society*, **17(1)**, 53–39.

6. Jawad, A. Q., Zinad, D. S., Salim, R. D., Al-Amiery, A. A., Gaaz, T. S., Takriff, M. S. and Kadhum, A. A. H. (2019) Synthesis, characterization, and corrosion inhibition potential of novel thiosemicarbazone on mild steel in sulfuric acid environment. *Coatings*, **9(11)**, 729–743.

7. Hazani, N. N., Dzulkifli, N. N., Sheikh Mohd Ghazali, S. A. I., Mohd, Y., Farina, Y. and Jamion, N. A. (2018) Synthesis, characterisation and effect of temperature on corrosion inhibition by thiosemicarbazone derivatives and its tin(IV) complexes. *Malaysian Journal of Analytical Sciences*, **22(5)**, 758–767.

8. Abbas, M. A., Bedair, M. A., El-Azabawy, O. E. and Gad, E. S. (2021) Anticorrosion effect of ethoxylate sulfanilamide compounds on carbon steel in 1M hydrochloric acid: electrochemical and theoretical studies. *ACS Omega*, **6(23)**, 15089–15102.

9. Mahdi, B. S., Abbass, M. K., Mohsin, M. K., Al-azzawi, W. K., Hanoon, M. M., Al-kaabi, M. H. H., Shaker, L. M., Al-amiery, A. A., Isahak, W. N. R. W., Kadhum, A. A. H. and Takriff, M. S. (2022) Corrosion inhibition of mild steel in hydrochloric acid environment using terephthaldehyde based on schiff base: gravimetric, thermodynamic, and computational studies. *Molecules*, **27(15)**, 4857–4875.

10. Rizal, R. M., Ali, H. M. and Ng, S. W. (2008) 1*H*-Indole-3-carbaldehyde thiosemicarbazone. *Acta Crystallographica Section E: Structure Reports*, **64(Pt 5)**, o919–o920.

11. Idelfitri, N. I. F., Dzulkifli, N. N., Ash'ari, N. A. N., Sapari, S., Abdul Razak, F. I. and Pungot, N. H. (2023) Synthesis, characterisation and corrosion inhibitory study of Meldrum's acid thiosemicarbazone: Weight Loss, SEM-EDX and DFT. *Inorganic Chemistry Communications*, **150**, 110485–110495.

12. Aziz, I. A. A., Abdulkareem, M. H., Annon, I. A., Hanoon, M. M., Al-Kaabi, M. H. H., Shaker, L. M., Alamiery, A. A., Isahak, W. N. R. W. and Takriff, M. S. (2022) Weight loss, thermodynamics, SEM, and electrochemical studies on *N*-2-methylbenzylidene-4- antipyrineamine as an inhibitor for mild steel corrosion in hydrochloric acid. *Lubricants*, **10(2)**, 23–39.

13. Hazani, N. N., Mohd, Y., Sheikh Mohd Ghazali, S. A. I., Farina, Y. and Dzulkifli, N. N. (2019) Electrochemical studies on corrosion inhibition behaviour of synthesised 2-acetylpyridine 4-ethyl-3-thiosemicarbazone and its tin(IV) complex for mild steel in 1 M HCl solution. *Journal of Electrochemical Science and Technology*, **10(1)**, 29–36.

14. Ouakki, M., Galai, M., Rbaa, M., Abousalem, A. S., Lakhrissi, B. and Cherkaoui, M. (2019) quantum chemical and experimental evaluation of the inhibitory action of two imidazole derivatives on mild steel corrosion in sulphuric acid medium. *Heliyon*, **5(11)**, E02759–E02776.

15. Becke, A. D. (1992) Density-functional thermoschemistry. I. The effect of the exchange-only gradient correction. *The Journal of Chemical Physics*, **96**, 2155–2160.

16. Frisch, M., Trucks, G., Schlegel, H., Scuseria, G., Robb, M., Cheeseman, J., Scalmani, G., Barone,

21 Intan Syahirah Abdul Salam, Sheikh Ahmad
    Izaddin Sheikh Mohd Ghazali, Siti Syaida
    Sirat and Nur Nadia Dzulkifli

Corrosion Inhibitory Evaluation of Indole-3-Carbaldehyde
4-Methyl-3-Thiosemicarbazone on Mild Steel: Weight,
Loss, Langmuir Isotherm, SEM-EDX and DFT Analysis

V., Mennucci, B. and Petersson, G. (2009) In
Gaussian 09, 32 (Gaussian Inc, Wallingford, CT)
5648.

17. Lee, C., Yang, W. and Parr, R. G. (1988)
Development of the colle-salvetti correlation-
energy formula into a functional of the electron
density. *Physical Review B: Condensed Matter
and Materials Physics*, **37(2)**, 785–789.

18. Lingling, L., Jie, Y., Zhigang, Z., Peiyu, S.
and Xingli, L. (2010) Solvent-free synthesis of
indole-based thiosemicarbazones under microwave
irradiation. *Journal of Chemical Research*, 57–60.

19. Suni, V., Kurup, M. R. P. and Nethaji, M. (2006)
Structural and spectral perspectives of a novel
thiosemicarbazone synthesized from di-2-pyridyl
ketone and 4-phenyl-3-thiosemicarbazide. *Spectro-
chimica Acta Part A: Molecular and Biomolecular
Spectroscopy*, **63(1)**, 174–181.

20. Gujarathi, J. R., Pawar, N. S. and Bendre, R. S.
(2013) Synthesis, spectral and biological study of
four and five co-ordinate copper (II) complexes
derived from 5-chloro-2-hydroxy acetophenone
N(4)-methyl thiosemicarbazone. *Der Pharma
Chemica*, **5(2)**:111–117.

21. Kavitha, E., Selvakumar, S., Chitra, A. and
Madhavan, J. (2016) Spectroscopic studies on
schiff base complex of NLO single crystal: BLZC.
International Journal of Physics, **2(1)**, 1–4.

22. Hossain, M. S., Zakaria, C. M., Kudrat-E-Zahan,
M. and Zaman, B. (2017) Synthesis, spectral and
thermal characterization of Cu(II) complexes with
two new Schiff base ligand towards potential
biological application. *Der Chemica Sinica*,
8(3), 380–392.

23. Lewis, N. A., Liu, F., Seymour, L., Magnusen,
A., Erves, T. R., Arca, J. F., Beckford, F. A.,
Venkatraman, R., González-Sarrías, A., Fronczek,
F. R., VanDerveer, D. G., Seeram, N. P., Liu, A.,
Jarrett, W. L. and Holder, A. A. (2011) Synthesis,
characterisation, and preliminary in vitro studies
of Vanadium(IV) complexes with a Schiff base
and thiosemicarbazones as mixed ligands. *European
Journal of Inorganic Chemistry*, **2012(4)**, 664–677.

24. Gunawan, R. and Nandiyanto, A. B. (2021) How
to read and interpret ^{1}H-NMR and ^{13}C-NMR
spectrums. *Indonesian Journal of Science &
Technology*, **6(2)**, 267–298.

25. Carrasco, F., Hernández, W., Chupayo, O., Álvarez,
C. M., Oramas-Royo, S., Spodine, E., Tamariz-
Angeles, C., Olivera-Gonzales, P. and Dávalos,
J. Z. (2020) Indole-3-carbaldehyde semicarbazone
derivatives: Synthesis, characterization, and

antibacterial activities. *Journal of Chemistry*,
2020, 1–9.

26. Qazi, S. U., Rahman, S. U., Awan, A. N., Al-
Rashida, M., Alharthy, R. D., Asari, A., Hameed,
A. and Iqbal, J. (2018) Semicarbazone derivatives
as urease inhibitors: synthesis, biological evaluation,
molecular docking studies and in-silico ADME
evaluation. *Bioorganic Chemistry*, **79**, 19–26.

27. Shakya, B. and Yadav, P. N. (2012) Synthesis
and characterization of 2-pyridineformamide 3-
pyrrolidinylthiosemicarbazone. *Journal of Nepal
Chemical Society*, **29**, 28–33.

28. Dzulkifli, N. N., Farina, Y., Mohd Yamin, B. and
Ibrahim, N. (2017) Synthesis, structural, chemical
properties, and anti-bacterial screening of Sm(III)
thiosemicarbazone complexes. *Malaysian Journal
of Analytical Sciences*, **21(3)**, 560–570.

29. Jayakumar, S. P., Murugadoss, V. and Angaiah,
S. (2021) Influence of electron releasing groups
in benzylidene thiocarbohydrazide and their
synergistic effect with iodide ions on acidizing
corrosion inhibition of carbon steel in 15% HCl
solution—experimental and theoretical approach.
Indian Journal of Chemical Technology, **28(4)**,
385–401.

30. Hashim, N. Z., Kahar, M. A., Kassim, K., Embong,
Z. and Anouar, E. H. (2020) Experimental and
theoretical studies of azomethines derived from
benzylamine as corrosion inhibitors of mild steel
in 1 M HCl. *Journal of Molecular Structure*,
1222, 128899- 1289911.

31. Aslam, R., Serdaroglu, G., Zehra, S., Kumar
Verma, D., Aslam, J., Guo, L., Verma, C., Ebenso,
E. E. and Quraishi, M. A. (2022) Corrosion
inhibition of steel using different families of
organic compounds: Past and present progress.
Journal of Molecular Liquid, **348**, 118373–
118401.

32. Ajeel, S. A., Waadulah, H. M. and Sultan, D. A.
(2012) Effects of H_2SO_4 and HCl concentration
on the corrosion resistance of protected low
carbon steel. *Al-Rafidain Engineering Journal*,
20(6), 1–7.

33. Akinbulumo, O. A., Odejobi, O. J. and Odekanle,
E. L. (2020) Thermodynamics and adsorption
study of the corrosion inhibition of mild steel by
Euphorbia heterophylla L. extract in 1.5 M HCl.
Results in Materials, **5**, 100074–100080.

34. Alias, N. A. A., Sheikh Mohd Ghazali, S. A. I.,
Sirat, S. S., Md Yusof, E. N., Sharif, I., Dzulkifli,
N. N. (2024) Synthesis and corrosion inhibitory
mechanism study of butyltin(IV) dithiocarbamate

22 Intan Syahirah Abdul Salam, Sheikh Ahmad
Izaddin Sheikh Mohd Ghazali, Siti Syaida
Sirat and Nur Nadia Dzulkifli

Corrosion Inhibitory Evaluation of Indole-3-Carbaldehyde
4-Methyl-3-Thiosemicarbazone on Mild Steel: Weight,
Loss, Langmuir Isotherm, SEM-EDX and DFT Analysis

in 1 M HCl: Weight loss, electrochemical, langmuir isotherm, surface and DFT analysis. *Polyhedron*, **252**, 116857–116873.

35. Humpola, D., Odetti, H. S., Fertitta, A. E. and Vicente, J. L. (2013) Thermodynamic analysis of adsorption models of phenol in liquid phase on different activated carbons. *Journal of the Chilean Chemical Society*, **58(1)**, 1–4.

36. Xu, B., Liu, Y., Yin, X., Yang, W. and Chen, Y. (2013) Experimental and theoretical study of corrosion inhibition of 3-pyridinecarbozalde thiosemicarbazone for mild steel in hydrochloric acid. *Corrosion Science*, **74**, 206–213.

37. Dharmendra, K. S., Eno, E. E., Mantu, K. S., Debasis, B., Udayabhanu, G. and Rohith P. J. (2018) Non-toxic schiff bases as efficient corrosion inhibitors for mild steel in 1 M HCl: electro-chemical, AFM, FESEM and theoretical studies. *Journal of Molecular Liquids*, **250**, 88–99.

38. John, S., Jeevana, R., Aravindakshan, K. K. and Joseph, A. (2017) Corrosion inhibition of mild steel by *N*-(4)-substituted thiosemicarbazone in hydrochloric acid media. *Egyptian Journal of Petroleum*, **26(2)**, 405–412.

39. Gebril, M. A., Bedair, M. A., Soliman, S. A., Bakr, M. F. and Mohamed, M. B. (2022) Experimental and computational studies of the influence of non-ionic surfactants with coumarin moiety as corrosion inhibitors for carbon steel in 1.0 M HCl. *Journal of Molecular Liquids*, **349**, 118445–118463.

40. Ermiş, E. (2018) Synthesis, spectroscopic characterization and DFT calculations of novel schiff base containing thiophene ring. *Journal of Molecular Structure*, **1156**, 91–104.

41. Tezcan, F., Yerlikaya, G., Mahmood, A. and Kardaş, G. (2018) A novel thiophene schiff base as an efficient corrosion inhibitor for mild steel in 1.0 M HCl: Electrochemical and quantum chemical studies. *Journal of Molecular Liquids*, **269**, 398–406.

42. Ranwa, N. L. S., Bavaliya, N. K. and Singh, H. L. (2017) Synthesis, characterization, DFT and antimicrobial studies on copper(II) complexes of nitrogen and sulphur donor ligands. *Journal of Innovative Research Clinical & Medical Sciences*, **1(2)**, 1–15.

43. Domingo, L. R., Aurell, M. J., Perez, P. and Contreras, R. (2002) Quantitative characterization of the global electrophilicity power of common diene/dienophile pairs in Diels-Alder reactions. *Tetrahedron*, **58**, 4417−4423.

44. Ani, F. E., Ibeji, C. U., Obasi, N. L., Kelani, M. T., Ukogu, K., Tolufashe, G. F., Ogundare, S. A., Oyeneyin, O. E., Maguire, G. E. M. and Kruger, H. G. (2021) Crystal, spectroscopic and quantum mechanics studies of Schiff bases derived from 4-nitrocinnamaldehyde. *Scientific Reports*, **11**, 8151–8161.

45. Touafri, L., Hellal, A., Chafaa, S., Khelifa, A. and Kadri, A. (2017) Synthesis, characterisation and DFT studies of three schiff bases derived from histamine. *Journal of Molecular Structure*, **1149**, 750–760.